Mobility Limited Flip-Based Sensor Networks Deployment

Sriram Chellappan, Xiaole Bai, Bin Ma, Dong Xuan, *Member*, *IEEE*, and Changqing Xu

Abstract—An important phase of sensor networks operation is deployment of sensors in the field of interest. Critical goals during sensor networks deployment include coverage, connectivity, load balancing, etc. A class of work has recently appeared, where mobility in sensors is leveraged to meet deployment objectives. In this paper, we study deployment of sensor networks using mobile sensors. The distinguishing feature of our work is that the sensors in our model have limited mobilities. More specifically, the mobility in the sensors we consider is restricted to a flip, where the distance of the flip is bounded. We call such sensors as *flip-based* sensors. Given an initial deployment of flip-based sensors in a field, our problem is to determine a movement plan for the sensors in order to maximize the sensor network coverage and minimize the number of flips. We propose a minimum-cost maximum-flow-based solution to this problem. We prove that our solution optimizes both the coverage and the number of flips. We also study the sensitivity of coverage and the number of flips to flip distance under different initial deployment distributions of sensors. We observe that increased flip distance achieves better coverage and reduces the number of flips required per unit increase in coverage. However, such improvements are constrained by initial deployment distributions of sensors due to the limitations on sensor mobility.

Index Terms—Sensor networks deployment, limited mobility, flip-based sensors.

1 Introduction

Sensor networks deployment in an important phase of sensor networks operation. A host of works has appeared in this realm in the recent past [1], [2], [3], [4], [5], [6], [7], [8], [9]. One of the important goals of sensor networks deployment is to ensure that the sensors meet critical network objectives that may include coverage, connectivity, load balancing, etc. When a number of sensors are to be deployed, it is not practical to manually position sensors in desired locations. In many situations, the sensors are deployed from a remote site (like from an airplane) that makes it very hard to control deployment.

To address this issue, a class of work has recently appeared where mobility of sensors is taken advantage of to achieve desired deployment [1], [2], [4], [7]. Typically, in such works, the sensors detect lack of desired deployment objectives. The sensors then estimate new locations and move to the resulting locations. While the above works are quite novel in their approaches, the mobility of the sensors in their models is unlimited. Specifically, if a sensor chooses to move to a desired location, it can do so without any limitation in the movement distance.

In practice, however, it is quite likely that the mobility of sensors is limited. Toward this extent, a class of Intelligent Mobile Land Mine Units (IMLM) [10] to be deployed across battlefields have been developed by DARPA. The IMLM units are expected to detect breaches and move to repair them. The mobility of the IMLM units is limited. Briefly, the mobility system in [10] is based on a hopping mechanism that is actuated by a single-cylinder combustion process. Each IMLM unit in the field carries onboard fuel tanks and a spark initiation/propeller system. For each hop, the fuel is metered into the combustion chamber and ignited to propel the IMLM unit into the air. The hop distance is limited depending on the amount of fuel and the propeller dynamics. The units include a righting and steering system for orientation during hops. Other technologies can also assist in such mobilities, like sensors enabled with spring actuation, external agents launching sensors after being deployed in the field, etc. Such a model typically trades off mobility for energy consumption and cost. In many applications, the latter goals outweigh the necessity for advanced mobilities, making such mobility models quite practical in the future.

In this paper, we study sensor networks deployment using sensors with limited mobilities. In our model, sensors can *flip* (or hop) only once to a new location and the flip distance is bounded. We call such sensors *flip-based* sensors. A certain number of flip-based sensors are initially deployed in the sensor network that is clustered into multiple regions. The initial deployment may not cover all regions in the network. Regions that do have any sensor in them are *holes*. In this framework, our problem is to determine an optimal movement (or flip) plan for the sensors in order to maximize the number of regions that is covered by at least one sensor (or minimize the number of holes) and simultaneously minimize the total number of sensor movements (or flips).

We propose a minimum-cost maximum-flow-based solution to our deployment problem. Our approach is to translate the sensor network at initial deployment and

- *S. Chellappan, X. Bai, and D. Xuan are with the Department of Computer Science and Engineering, The Ohio State Univeristy, 395 Dreese Laboratories, 2015 Neil Avenue, Columbus, OH 43210-1277. E-mail: {chellapp, baixia, xuan}@cse.ohio-state.edu.*
- *B. Ma is with the Department of Computer Science, Middlesex College 366, University of Western Ontario, London, ON, Canada, N6A 5B7. E-mail: bma@csd.uwo.ca.*
- *C. Xu is with the Department of Electronic Engineering, Shanghai Jiao Tong University, 1954 Huashan Road, Shanghai, 200030, P.R. China. E-mail: cqxu@sjtu.edu.cn.*

Manuscript received 1 June 2005; revised 26 Sept. 2005; accepted 29 Oct. 2005; published online 27 Dec. 2005.
Recommended for acceptance by M. Ould-Khaoua.
For information on obtaining reprints of this article, please send e-mail to: tpds@computer.org, and reference IEEECS Log Number TPDS-0270-0605.

sensor mobility model into a graph (called *virtual graph*). Regions in the sensor network are modeled as vertices and possible sensor movement paths between regions are modeled as edges between corresponding vertices in the virtual graph. Capacities for the edges model the number of sensors that can flip between regions. A cost value is also assigned to the edges to capture the number of flips between regions. Since the virtual graph models the sensor network, our problem of optimally moving sensors to holes can be translated as one where we want to optimally determine flows to hole vertices in the virtual graph. The first objective of our problem, namely, determining a movement plan to maximize coverage, can be translated as determining the flow plan (a set of flows in the virtual graph) that corresponds to the maximum flow to hole vertices in the virtual graph without violating edge capacities. Note that there can be more than one flow plan that can maximize the flow in the virtual graph. Out of such flow plans, our second objective is to determine the plan that minimizes the overall cost, which corresponds to the minimizing the number of sensor flips. Intuitively, each flow in the flow plan (in the virtual graph) denotes a path for a sensor movement to a hole in the sensor network. As we discuss later, the maximum flow value in the virtual graph denotes the maximum number of holes into which a sensor can move without violating the mobility constraints, while the minimum cost denotes the corresponding minimum number of sensor movements (or flips).[1]

In our solution, we translate the flow plan corresponding to the minimum cost maximum flow in the virtual graph into a movement plan for the sensors in the region. We subsequently prove the optimality of this movement plan. We also propose multiple approaches that sensors can adopt to execute our solution in practice. We then perform simulations to study the sensitivity of coverage and the number of flips to flip distance under different initial deployment distributions of sensors. We observe that increased flip distance achieves better coverage and reduces the number of flips required per unit increase in coverage. However, such improvements are constrained by initial deployment distributions of sensors due to the limitations on sensor mobility.

The rest of our work is organized as follows: We present important related work in Section 2. In Section 3, we formally define our flip-based mobility model and our deployment problem. We then present our solution, its properties, and alternate approaches to execute our solution in Section 4. In Section 5, we present results of our performance evaluations. We present some discussions in Section 6 and conclude our paper with some final remarks in Section 7.

2 Related Work

Sensor network deployment is a topic that has received significant attention in the recent past [1], [2], [3], [4], [5], [6], [7], [8], [11], [12], [9] [13]. In this section, we focus on works related to mobility assisted sensor networks deployment [1], [2], [4], [7]. The key objective in [1], [4], [7] is to detect holes in the network and cover them with at least one sensor. In the approach proposed by Wang et al. in [4] the detection of holes is based on constructing Voronoi diagrams. Each sensor constructs its own Voronoi polygon, which enables sensors to detect holes. The authors then propose three algorithms, namely, Vector-based algorithm, Voronoi-based algorithm, and Minimax algorithm to maximize coverage. In their algorithms, sensors move over a series of iterations to balance virtual forces between themselves. They stop moving when global force balance is achieved, which corresponds to attainment of desired deployment. In [1], Howard et al. propose the idea of constructing potential fields to maximize coverage. The fields are constructed such that each node is repelled by both obstacles and by other nodes, thereby forcing the sensors to spread throughout the environment. In Zou and Chakrabarty's work in [7], all sensors in the network forward their location to a centralized node. The centralized node determines the final positions of sensors as those positions that balance the virtual forces in the network.

In all the above works [1], [4], [7], sensors move depending on virtual forces exerted by them. In the principle of virtual forces, sensors attract each other if they are far apart and repel each other if they are too close. In this approach, sensors keep moving over several iterations. In each iteration, a degree of force balance is achieved by the sensors. After many such iterations, sensors achieve global force balance among themselves, which in turn corresponds to attainment of desired deployment objectives. The virtual force approach cannot work for our problem for two reasons. Sensors in our model are capable of only a *flip*. The lack of *continuous* motion implies that, even between two sensors, force balance may not be achieved if they flip toward or apart from each other. Second, the virtual force approach requires a series of iterations (a series of sensor movements) to achieve global force balance in the network. When constrained by mobility, the virtual force approach has limited application.

Another related work is Wu and Yang's work in [2]. In [2], the sensor network is divided into clusters. The objective is to ensure that the number of sensors per cluster is uniform. The algorithms designed efficiently scan the clusters in two stages (row-wise and column-wise) sequentially and determine new sensor locations (or clusters) in each stage. Sensors move in each stage to new clusters to achieve uniform deployment. Intuitively, this approach has some applicability to our problem. Sensors can exchange information row-wise (along all rows) and then flip between regions in their row first. A column-wise information exchange and flip can follow next. Clearly, coverage is improved here compared to initial deployment. However, the final deployment in the two-stage approach will be far from optimal in terms of both coverage and sensor flips. Optimizing coverage sequentially in row-wise and column-wise directions results in nonoptimal flips that will compromise optimality of final coverage. Due to the two-stage flip sequence for sensors (row-wise and column-wise), more than necessary flips can be introduced.

To summarize here, our objectives in this paper (maximizing coverage and minimizing sensor movements) shares similarities with the above works [1], [2], [4], [7]. The major

1. The translation will become clearer once we discuss exactly how capacities and costs are assigned in the virtual graph in Section 4.2.

reason why the above approaches do not work in our problem is due to limitations on sensor mobility. In the above works, sensors move based on local measurements and communications. Erroneous movements made by the sensors are eventually corrected over time since the sensor movement distance is unlimited. In our problem, sensor movement distance itself is a hard constraint. This means that we are fundamentally constrained by the movement choices available to us (compared to unlimited mobility) during deployment. The consequence is the increased importance that each sensor flip needs to be accorded. Sensors therefore cannot just make local decisions and flip. We need to determine a *movement plan* for the sensors prior to their flip, which is the output of our solution in this paper.

3 Mobility Model and Problem Definition

3.1 The Flip-Based Sensor Mobility Model

In this paper, we model sensor mobilities as a *flip*. That is, the motion of the sensor is in the form of a flip (or hop) from its current location to a new one when triggered by an appropriate signal. Such a movement can be realized in practice by propellers powered by fuels [10], coiled springs unwinding during flips, external agents launching sensors after being deployed in the field, etc. In our model, sensors can flip only once to a new location. This could be due to propeller dynamics or the spring being unable to recoil after a flip or the external agent launching the sensor. The distance to which a sensor can flip is limited. The sensor can flip in a desired angle. Mechanisms in [10] can be used for orientation during flips. The limitation in sensor mobility comes from the bound on the maximum distance they can move, which again depends on available fuel quantity, degree of spring coil, etc. We study two models of flip-based mobility. The first is a fixed distance mobility model, while the second is a variable distance mobility model.

We denote the maximum distance a sensor can flip to as F. In the first model, the distance to which a sensor can flip is fixed and is equal to F. We extend the above model further. Although the number of flips is still one, in many cases, depending on the triggering signals, fuel can be metered variably or the spring can unwind only partially or the external agent can variably adjust the flip distance during launching. In the second model, sensors can flip to distances between 0 and F. We denote d as the basic unit of distance flipped. We assume that F is an integral multiple of the basic unit d. Thus, in the second model, sensors can flip once to distances d, $2d$, $3d$, $\dots nd$ from its current location, where $nd = F$. To differentiate the above two models, we introduce the notation C to denote *choice* for flip distance. $C = 1$ denotes the first model, where the sensor has only one fixed choice for flip distance (the maximum distance F). $C = n$ denotes the second model, where the sensor has n choices for the flip distance (between d and maximum distance F). For the rest of the paper, unless otherwise clearly specified, the term flip distance denotes the maximum flip distance F.

3.2 Problem Definition

The sensor network we study is a square field. It is divided into two-dimensional regions, where each region is a square of size R. A certain number of flip-based sensors are deployed initially in the network. The initial deployment may have *holes* that are not covered by any sensor. In this context, our problem statement is: Given a sensor network of size D, a desired region size R, an initial deployment of N flip-based sensors that can flip once to a maximum distance F, our goal is to determine an optimal movement plan for the sensors in order to maximize the number of regions that is covered by at least one sensor, while simultaneously minimizing the total number of flips required. The input to our problem is the initial deployment (number of sensors per region) in the sensor network and the mobility model of sensors. The output is the detailed movement plan of the sensors across the regions (which sensors should move and where) that can achieve our desired objectives.

The region size R is contingent on the application, based on the sensing/transmission ranges of sensors and application demands. We assume that $min\{\frac{S_{sen}}{\sqrt{2}}, \frac{S_{tr}}{\sqrt{5}}\} \geq R$, where S_{sen} and S_{tr} are sensing and transmission ranges of the sensors, respectively. This guarantees that if a sensor is present in a region, every point in the region is *covered* by the sensor and the sensor can communicate with sensors in each of its four adjacent regions. In this paper, we first assume that the desired region size R is an integral multiple of the basic unit of flip distance, i.e., $R = m * d$, where m is an integer ($\geq$ 1). We discuss the general case of R subsequently in Section 6. We assume that each sensor knows its position. To do so, sensors can be provisioned with GPS devices, or approaches in [14] can be applied, where sensors are localized using sensors themselves as landmarks. In our model, the regions to which a sensor can flip are those in its left, right, top, and bottom directions. However, those regions need not be just the adjacent neighbors. They depend on the flip distance F. After discussing the above case, the general case, where a sensor can flip to regions in any arbitrary direction is discussed subsequently in Section 6. The base-station can reside anywhere as long as it is able to communicate with the sensors.

3.3 An Example

We illustrate our problem further with an example. Fig. 1a shows an instance of initial deployment in the sensor network. The shaded circles denote sensors and the numbers denote the id of the corresponding region in the network. The neighbors of any region are its immediate left, right, top, and bottom regions. For instance, in Fig. 1, the neighbors of region 6 are regions 2, 5, 7, and 10. In Fig. 1a, after the initial deployment, regions 1, 6, 11, 12, and 16 are not covered by any sensor and are thus holes. Optimally covering such holes is the problem we address in this paper.

The above problem is not easy to solve. For instance, consider Fig. 1a. For ease of elucidation, let the desired region size $R = d$. Let the flip distance $F = d$. One intuitive approach toward maximizing coverage is to let sensors from source regions (more than one sensor) to flip to hole regions (no sensors) in their neighborhood, using local information around them. In Fig. 1a, region 7 has three sensors in it, while region 11, a neighbor of 7, is empty. Similarly, region 8 has a sensor, while its neighbor, region 12, is empty. If we allow neighbors to obtain local neighbor information, then, intuitively, a sensor from region 7 will attempt to cover regions 11

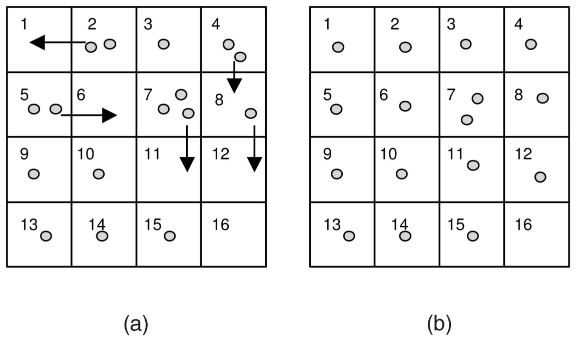

Fig. 1. (a) A snapshot of the sensor network and a movement plan to maximize coverage and (b) the resulting deployment.

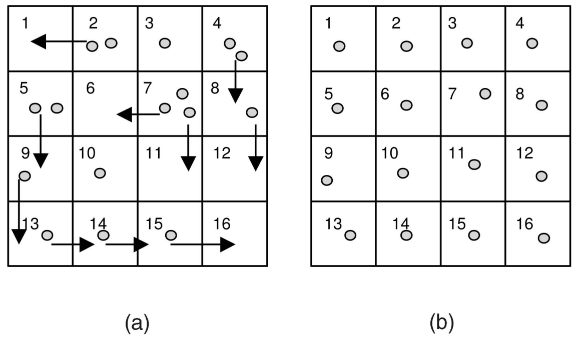

Fig. 2. (a) A snapshot of the sensor network and the optimal movement plan and (b) the resulting deployment.

and 16. This intuition is because region 7 (with extra sensors) is nearest to holes 11 and 16. Similarly, region 4 will try to cover region 12. The resulting sequence of flips and the corresponding deployment are shown in Figs. 1a and 1b, respectively.

With this movement plan, region 16 is still uncovered, as shown in Fig. 1b. This is because, while region 7 has extra sensors, there are no mobile sensors in regions 11 and 12 (that can flip further). Also, region 15 cannot provide a sensor without making itself (or some other region) a hole. This means that all paths to region 16 are *blocked* in this movement plan, preventing region 16 from being covered. However, there exists an optimal plan that can cover all regions in this case, as shown in Fig. 2. For optimal deployment, the path of movements to cover region 16 incurs a *chain* of flips starting from region 5 toward region 16. In fact, for optimal coverage, this plan also requires the minimum number of flips (10 flips). The key challenges we have to overcome to solve our problem are 1) the trade-offs in simultaneously attempting to optimize both coverage and number of flips and 2) the constraints arising from limited mobility, due to which a sensor from a far away region may need to flip toward a far away hole and a *chain* of flips may need to progressively occur toward the particular hole for covering it. Determining such a movement plan for optimizing both coverage and number of flips is not trivial.

4 Our Solution

4.1 Design Rationale

In this paper, we propose a solution where information on the number of sensors per region for all regions is collected by the base-station and an optimal movement plan for the sensors is determined and forwarded to the sensors. We propose a minimum-cost maximum-flow-based solution that is executed by the base-station using the region information to determine the movement plan. The base-station will then forward the movement plan (which sensors should move and where) to corresponding sensors in the network.

Each sensor in the network will first determine its position and the region it resides in. Sensors then forward their location information to the base-station.[2] The packets are forwarded toward the base-station through other neighboring regions closer to the base-station. To do so, protocols like [15], [16], [17] can be used, where the protocols route packets toward sinks in the network (the base-station in our case) using shortest paths. Another solution that does not require a centralized node is to let individual sensors collect region information and execute our solution independently to determine the movement plan. We discuss the latter solution in Section 4.5.

We now discuss how to translate our problem into a minimum-cost maximum-flow problem. Let us denote regions with at least two sensors as *sources*. Source Regions can provide sensors (like region 5 in Fig. 1a) or they can be on a path between another source and a hole. Let us denote regions with only one sensor as *forwarders*. Forwarder regions cannot provide sensors (otherwise, they become holes themselves), but they can be on a path between a source and a hole (like regions 9, 13, 14, and 15 in Fig. 1a). Let us denote regions without any sensor as *holes*. Obviously, holes can only accept sensors (regions 1, 6, 11, 12, and 16). The first objective of our problem is to maximize the number of holes that eventually have a sensor in them. Since there can be multiple sources and multiple forwarders, in the event of maximizing the number of holes that eventually contain a sensor, there can be many possible sequences of sensor movements. Out of such possible sequences, our second objective is to find the sequence that minimizes the number of sensor movements.

If we identify regions (sources, forwarders, and holes) using vertices and incorporate path relationships in the sensor network as edges (with appropriate constrained capacities) between the vertices, then, from a graph-theoretic perspective, our problem is a version of the multicommodity maximum flow problem, where the problem is to maximize flows from multiple sources to multiple sinks in a graph, while ensuring that the capacity constraints on the edges in the graph are not violated. While obtaining the optimal plan to maximize coverage, we also want to minimize the number of flips. That is, if we associate a cost with each flip, we wish to minimize the overall cost of flips while still maximizing coverage. This problem is then a version of the minimum-cost multicommodity maximum-flow problem, where the objective is to find paths that minimize the overall cost while still maximizing the flow. Our solution is to model the sensor network as an appropriate graph structure (called *virtual graph*) following the objectives discussed above, determine the minimum cost maximum flow plan in the virtual graph.

2. Alternatively, a region-head can be elected in each region to collect and forward information on the number of sensors in their region.

Each flow in the flow plan (in the virtual graph) denotes a path for a sensor movement from a source to a hole in the sensor network. As we discuss later, the maximum flow value in the virtual graph denotes the maximum number of holes into which a sensor can move without violating the mobility constraints, while the minimum cost denotes the corresponding minimum number of sensor movements (or flips). We then translate the flow plan as flip sequences in the sensor network. For the rest of the paper, if the context is clear, we will call our solution as minimum-cost maximum-flow solution.

4.2 Constructing the Virtual Graph from the Initial Deployment

We now discuss the construction of the virtual graph in detail. The inputs are the initial deployment (with N sensors), the granularity of desired coverage (region size R), flip distance (F), and the number of sensors per region i (n_i). We denote the number of regions in the network as Q. Let $G_S(V_S, E_S)$ be an undirected graph representing the sensor network. Each vertex $\in V_S$ represents one region in the sensor network and each edge $\in E_S$ represents the path relationship between regions. G_S purely represents the initial network structure (and does not reflect whether regions are sources, forwarders, or holes) and as such is undirected. The virtual graph (denoted by $G_V(V_V, E_V)$) is constructed from G_S.

The key task in constructing the virtual graph (G_V) is to first determine its vertices (the set V_V) commensurate with the status of each region as a source, forwarder, or hole. Then, we have to establish the edges (the set E_V), directions, capacities, and costs in G_V between the vertices. For any region i in the sensor network, we denote its *reachable* regions as those to which a sensor from region i can flip to. Obviously, the reachable regions depend on the flip distance F. In G_V, edges are added between such reachable regions. The directions of edges between vertices are based on whether the corresponding regions are sources, forwarders, or holes in the sensor network. The capacities of the edges depend on the number of sensors in the regions, while the cost is used to quantify the number of sensor flips between regions in the sensor network. We denote $C(p, q)$ as the capacity and $Cost(p, q)$ as the cost of the edge between vertices p and q in G_V, respectively. The final objective is to ensure that the minimum-cost maximum-flow plan in G_V can be translated into an optimal movement (flip) plan for sensors in the network. In the following, we first discuss how to construct the virtual graph for a simple, yet representative basic case. We then discuss how to construct the virtual graph for general case.

4.2.1 Constructing the Virtual Graph for the Case $R = d$

In this case, the region size R is equal to the basic unit of flip distance d. To explain the virtual graph construction process clearly, we first describe it for the case where the flip distance $F = d$, and $C = 1$. That is, the flip distance is the basic unit d and the sensor has only one choice for flip distance. We discuss the case where $F > d$ and $C = 1$, and $F > d$ and $C = n$ (multiple choices) subsequently. The case where $R > d$ is discussed in Section 4.2.2.

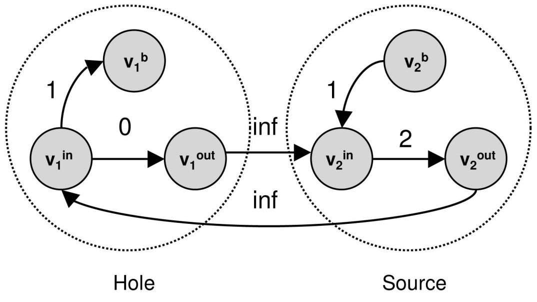

Fig. 3. The virtual graph with only regions 1 and 2 in it.

Construction when $F = d$ **and** $C = 1$. In the virtual graph, each region (of size R) is represented by three vertices. For each region i, we create a vertex for it in G_V called base vertex, denoted as v_i^b. The base vertex v_i^b of region i keeps track of the number of sensors that are in region i. For each region, we need to keep track of the number of sensors from other regions that have flipped to it and the number of sensors that have flipped from this region to other regions. The former task is accomplished by creating an in vertex and the latter is accomplished by creating an *out* vertex for each region. For each vertex i, its *in* vertex in the virtual graph is denoted as v_i^{in} and its *out* vertex is denoted as v_i^{out}.

Having established the vertices, we now discuss how edges (and their capacities) are added between vertices in G_V. Recall that each region that has $\geq$ 2 sensors is considered a source and each region that has $\geq$ 1 sensor is considered a forwarder. We are interested in how to optimally *push* sensors from such regions. For such regions, an edge is added from the corresponding v_i^b to v_i^{in} with capacity $n_i - 1$. The interpretation of this is that, when attempting to determine the flow from the base vertex (v_i^b), at least one sensor will remain in the corresponding region i. Then, an edge with capacity n_i is added from the same v_i^{in} to v_i^{out}. This ensures that it is possible for up to n_i sensors in this region to flip from it. Recall the example in Fig. 1a. Region 2 is a source. The G_V construction corresponding to this region is shown in Fig. 3, where there is an edge with capacity $n_2 - 1 = 1$ from vertex v_2^b to v_2^{in} and an edge of capacity $n_i = 2$ from v_2^{in} to v_2^{out}. Other source and forwarder regions are treated similarly in G_V.

Each region that has zero sensors is considered a hole. We are interested in how to optimally *absorb* sensors in such regions. For holes, an edge is added from the corresponding v_i^{in} to base vertex v_i^b with edge capacity equal to 1. This is to allow a maximum of one sensor into the base vertex v_i^b of hole region i. If a sensor flips to this hole, the hole is then covered and no other sensor needs to flip to this region. Then, an edge with capacity 0 is added from the same v_i^{in} to v_i^{out}. This is because a sensor that moves into a hole will be not able to flip further.[3] Recall again, from the example in Fig. 1a, that region 1 is a hole. In Fig. 3, there is an edge with capacity 1 from vertex v_1^{in} vertex to v_1^b and an edge of capacity 0 from v_i^{in} to the v_1^{out}. Other holes are treated similarly in G_V. We now have

3. In practice, an edge with capacity 0 need not be *specifically* added. We do so to retain the symmetricity in the virtual graph construction.

$$\forall v_i^{in} \quad and \quad v_i^{out} \in V_V, \quad C(v_i^{in}, v_i^{out}) = n_i, \tag{1}$$
$$\forall v_i^{b} \quad and \quad v_i^{in} \in V_V | n_i > 0, \quad C(v_i^{b}, v_i^{in}) = n_i - 1, \tag{2}$$
$$\forall v_i^{in} \quad and \quad v_i^{b} \in V_V | n_i = 0, \quad C(v_i^{in}, v_i^{b}) = 1. \tag{3}$$

The final step is to incorporate the *reachable* relationship that holds in the original deployment field into the virtual graph. Recall that, for any region i in the sensor network, its *reachable* regions are those regions to which a sensor from region i can flip to, which is determined by the flip distance (F). We have to incorporate this in the virtual graph. To do so, an edge of infinite capacity (denoted by *inf*) is added from v_i^{out} to v_j^{in} and another edge of infinite capacity is added from v_j^{out} to v_i^{in} if regions i and j are reachable from each other. This is to allow any number of flips between reachable regions if there are sensors in them. In Fig. 3, regions 1 and 2 are reachable from each other since $R = d$ and $F = d$. Thus, edges with infinite capacity are added from the v_1^{out} to v_2^{in} and from v_2^{out} to v_1^{in}. Formally, for all regions i and j that are reachable from each other in the sensor network, we have

$$C(v_i^{out}, v_j^{in}) = C(v_j^{out}, v_i^{in}) = inf. \tag{4}$$

Having discussed the capacity among edges, we now incorporate costs for each flow in G_V. If a flip occurs from some region i to some region j in the sensor network, we consider that a cost of one has incurred. From (4), we can see that the flips between reachable regions (say i and j) in the sensor network is translated in G_V by an edge from v_i^{out} to v_j^{in} and from v_j^{out} to v_i^{in}. In order to capture the number of flips between these regions, we add a cost value to these corresponding edges in G_V with cost value equal to 1. Let us denote $Cost(i, j)$ as the cost for a flip between vertices i and j. Formally, for all regions i and j that are reachable from each other in the sensor network, we thus have

$$Cost(v_i^{out}, v_j^{in}) = Cost(v_j^{out}, v_i^{in}) = 1. \tag{5}$$

The $Cost$ for other edges in G_V is 0. This is because, from the view of the sensor network, the edges, apart from those between *out* and *in* vertices across regions, are internal to a region. They cannot be counted toward sensor flips (which only occurs across regions). Instances of such edges are those from v_1^{in} to v_1^{b}, from v_1^{in} to v_1^{out} in Fig. 3. An instance of original deployment and the corresponding virtual graph at the start are shown in Figs. 4a and 4b, respectively. In Fig. 4a, the numbers denote the id of the corresponding region. We do not show the $Cost$ values in the virtual graph in Fig. 4b.

Construction when $F > d$ **and** $C = 1$. In the above, we discussed G_V construction for the case where $R = d$, $F = d$, and $C = 1$. When $F > d$ and $C = 1$, only the *reachability* relationship changes. Specifically, immediate neighboring regions are not reachable anymore from each other like in the case where $F = d$. When $F > d$, regions beyond immediate neighboring regions become reachable (depending on F). In G_V, edges of infinite capacity are added from v_i^{out} to v_j^{in} and from v_j^{out} to v_i^{in} if regions i and j are reachable from each other. For example, if $F = 2d$ and $C = 1$ in Fig. 4, the reachable regions for region 1 are regions 3 and 9 only. Thus, edges are created from v_1^{out} to v_3^{in} and v_9^{in} and from v_3^{out} and v_9^{out} to v_1^{in}. Other edges in G_V are modified similarly.

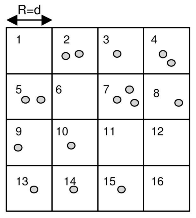

(a)

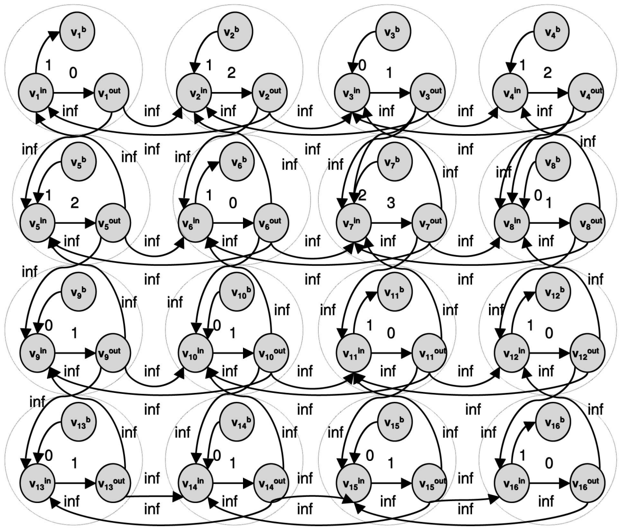

(b)

Fig. 4. (a) The initial sensor network deployment and (b) the corresponding virtual graph at the start in Case $R = d$.

The edge capacities ($C(i, j)$) and costs ($Cost(i, j)$) can be obtained following from discussions in Section 4.2.1.

Construction when $F > d$ **and** $C = n$. In this case again, only the reachability relationship changes. Recall that if $F > d$ and $C = n$, the distance of flip can be d, $2d$, $3d$, $\ldots nd$, where $F = nd$. For example, if $F = 2d$ and $C = 2$ in Fig. 4, then the reachable regions of region 1 are regions 2, 3, 5, and 9. Thus, apart from existing edges, edges are also added from v_1^{out} to v_3^{in} and v_9^{in} and from v_3^{out} and v_9^{out} to v_1^{in}. Other edges, capacities, and costs are modified similarly.

4.2.2 Constructing the Virtual Graph for the Case $R > d$

In this case, the region size $R > d$. We first describe the virtual graph construction for when the R is an integral multiple of d, i.e., $R = x \times d$, where x is an integer ($\geq$ 1),[4] $F = d$, and $C = 1$. For instance, if $x = 2$, then the requirement is to maximize number of regions (of size $2d$) with at least one sensor. Note that if $R = x \times d$, then there are x^2 subregions in each region. This is shown in Fig. 5a, where the region ($R = 2d$) is the area contained within dark borders. We denote each area within the shaded lines as subregions. Each subregion has a size d. The id of the regions is the number in bold at the center of the region. For ease of understanding, we keep the id of the subregions in Fig. 5. To explain construction

4. We discuss the general case of R in Section 6.

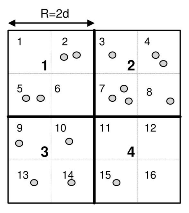

(a)

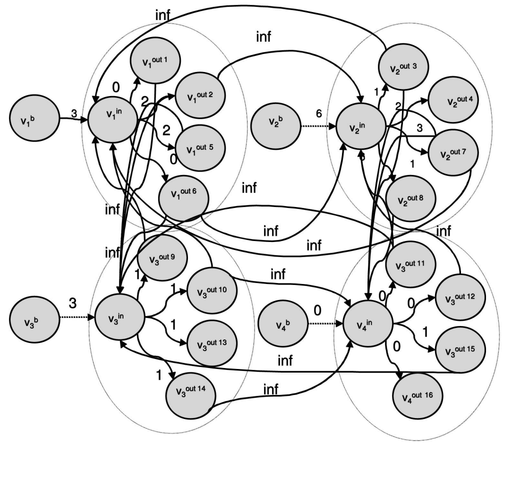

(b)

Fig. 5. (a) The initial sensor network deployment and (b) the corresponding virtual graph at the start in Case $R > d$.

process better, we say that a region i represents its subregions. In Fig. 5, region 1 is a representative of subregions 1, 2, 5, and 6.

In the virtual graph, each region (of size R), whose id is i, has a vertex v_i^b. For each region, we are interested in how many sensors from other subregions have flipped to it. Despite covering multiple subregions, we are interested in coverage of the region in itself (and not the subregions). Thus, we still need only one *in* vertex (v_i^{in}) for each region. However, each region has multiple subregions and sensors in them can be pushed out. Thus, the number of *out* vertices per region is equal to the number of subregions as shown in Fig. 5b. Note that sensors do not need to make internal flips to other subregions within a region as there is no improvement in region coverage. Hence, there are no edges created for internal flips within a region.

We now discuss how edges are added between vertices in G_V. Each region i that has ≥ 1 (or $= 1$) sensors is a source region (or a forwarder region) and an edge is added from v_i^b to v_i^{in} with edge capacity equal $\sum_{j=1}^{x^2} n_j - 1$ in the virtual graph, where x^2 is the number of subregions in each region and n_j is the number of sensors in subregion j. For example, in Fig. 5, region 1 is a source and there is an edge with capacity $\sum_{j=1}^{4} n_j - 1 = 3$ from vertex v_1^b to v_1^{in}. This ensures that, when determining the flow from this region, at least one sensor remains. Then, edges with capacity n_k are added from this v_i^{in} to each v_i^{outk}, as shown in Fig. 5, where v_i^{outk} is the *out* vertex corresponding to subregion k in region i. For each hole j, we add an edge with capacity 1 from the v_j^{in} vertex to v_j^b, an edge of 0 capacity from v_j^{in} to each v_j^{outk} in the virtual graph. Finally, to incorporate the reachability relationship between regions, an edge of infinite capacity is added from v_i^{outm} to v_j^{in} and an edge of infinite capacity is added from v_j^{outp} to v_i^{in} if regions i and j are reachable from each other *and* subregion m is reachable from region j and subregion p is reachable from region i as shown in Fig. 5. The cost that captures number of flips between regions is 1 between the corresponding edges above. Other edges that are between regions also have cost value 1. For each region i, the edges from v_i^b to v_i^{in} and from v_i^{in} to v_i^{outk} (for all k) do not count toward sensor flips and have 0 cost (similar to the preceding case). We can obtain equations for capacities and costs following from discussions in Section 4.2.1 in the preceding case. An instance of original deployment and the corresponding virtual graph at the start are shown in Figs. 5a and 5b, respectively. We do not show the cost values in the virtual graph in Fig. 5b.

The extensions to construct G_V when $F > d$ and $C = 1$ and when $F > d$ and $C = n$ for the case where $R > d$ are similar to those proposed for $F > d$ and $C = n$, and $F > d$ and $C = 1$, respectively, for the case where $R = d$. Due to space limitations, we do not describe the construction for these cases.

4.3 Determining the Optimal Movement Plan from the Virtual Graph

Recall that the base vertex (v_i^b) keeps track of the number of sensors in region i in G_V. Also, the edges going into the base vertices of holes have capacity *one* to allow a maximum of *one* sensor into the holes. Consequently, our problem can be translated as determining flows from the base vertices of source regions to as many base vertices of holes as possible in G_V, with minimum overall cost. Let us now discuss why this is true. From the construction rules of G_V, we can see that, for each feasible sensor movement sequence in the sensor network between a source region and a hole, there is a feasible path for a flow in G_V between base vertices of the corresponding regions and vice versa. For example, consider a feasible sensor movement sequence from a source region (say i) to a hole (say j) through forwarder regions $k, l, \ldots, m$ and n. We denote the path as a tuple of the form $< i, k, l, \ldots, m, n, j >$. The feasibility of this path means that each of regions $i, k, l, \ldots, m, n$ have at least one sensor in them and region i has at least two sensors. From the construction of G_V, the capacities $C(v_i^b,\ v_i^{in})$, $C(v_i^{in},\ v_i^{out})$, $C(v_i^{out}, v_k^{in})$, $C(v_k^{in}, v_k^{out})$, $C(v_k^{out}, v_l^{in})$, $\ldots, C(v_m^{out}, v_n^{in})$, $C(v_n^{in}, v_n^{out})$, $C(v_n^{out}, v_j^{in})$, and $C(v_j^{in}, v_j^b)$ are all ≥ 1 (where $C(i, j)$ was defined in Section 4.2.1). Thus, a flow from v_i^b to v_j^b is feasible in G_V.[5] The cost of this flow is the summation of the cost of all edges in the path. Recall that the cost of edges from *out* to *in* of reachable regions is one and all other edges costs are zero. Consequently, the cost of the above flow in G_V is the number of times a flow occurs between *out* and *in* vertices of successive reachable regions in the path. Clearly, this is the number of regions traversed in the sensor network (i.e., the number of flips). At this point, it is clear that if we can determine a flow plan

5. A similar argument can show that, for every feasible flow in G_V, a corresponding sensor movement sequence is feasible in the sensor network.

(the actual flow among the edges) in G_V that can maximize the flow from the base vertices of source regions to as many base vertices of holes with minimum overall cost, we can translate the flow plan as a movement plan for sensors (across the regions) in the sensor network that maximizes coverage and minimizes the number of sensor flips.

Determining the minimum cost maximum flow plan in a graph is a two step process. First, the maximum flow value from sources to sinks in the graph is determined (for which there are many existing algorithms). Second, the minimum cost flow plan (for this maximum flow) in the graph is determined (for which there are also many existing algorithms). In our implementations, we first determine the maximum flow value in G_V from all base vertices of source regions to base vertices of hole regions using the Edmonds-Karp algorithm [18]. We then determine the minimum cost flow plan (for the above maximum flow) in G_V using the method in [19], which is an implementation of the algorithm in [20]. For more details on the algorithms, readers can refer to [18], [19], and [20]. The corresponding flow plan is a set of flows in all edges in G_V corresponding to the minimum cost maximum flow in G_V.

Let W^V denote the flow plan (a set of flows) corresponding to the minimum cost maximum flow in G_V, where the amount of each flow is *one*. Each flow in W^V is actually a path from the base vertex of a source to the base vertex of a hole. The flow value is *one* for each flow since only one sensor eventually moves to a hole (from our problem definition). Consequently, the value of the maximum flow is the number of such flows (with flow value *one*), which in turn is the maximum number of holes that can be covered eventually with *one* sensor. Each flow $w^V_{i,j} \in W^V$ is a flow from the base vertex of a source v^b_i to the base vertex of a hole v^b_j in G_V and is of the form

$$\langle v^b_i, v^{in}_i, v^{out}_i, v^{in}_k, v^{out}_k, v^{in}_l, v^{out}_l, \ldots, v^{out}_m, v^{in}_n, v^{out}_n, v^{in}_j, v^b_j \rangle,$$

which denotes that the path of the flow is from v^b_i to v^{in}_i, from v^{in}_i to $v^{out}_i \ldots$, from v^{in}_j to v^b_j. From the construction of G_V, for each such $w^V_{i,j}$ ($\in W^V$), a corresponding movement sequence in the sensor network $w^S_{i,j}$ can be determined and is of the form $\langle r_i, r_k, r_l \ldots r_m, r_n, r_j \rangle$, where $r_i, r_k, r_l \ldots r_m, r_n, r_j$ correspond to regions $i, k, l, \ldots, mn, j$ in the sensor network, respectively. Physically, this means that one sensor should flip from regions i to k, k to $l, \ldots m$ to n and n to j. The sensor flip (or movement) plan W^S (set of all $w^S_{i,j}$) is the output of our solution.

Once the base-station determines the flip plan, it will forward instructions to the sensors (that need to flip). For each sensor, the base-station can forward instructions on the reverse direction of the original path of communication between the sensor and the base-station. The forwarded packet contains the destination of the sensor and the intended region the sensor needs to flip to. Since sensors know the regions they reside in, they can determine the direction of the intended region (i.e., left, right, top, or bottom region). We assume that sensors are equipped with steering mechanisms (similar to the one in [10]) that allow sensors to orient themselves in an appropriate direction prior to their flip. Theorem 1 shows that the flip plan obtained by our solution optimizes both coverage and the number of flips.

Theorem 1. *Let W^V_{opt} be the minimum-cost maximum-flow plan in G_V. Its corresponding flip plan W^S_{opt} will maximize coverage and minimize the number of flips (refer to the Appendix for the proof).*

We now discuss the time complexity of our solution. There are three phases in our solution while determining the optimal movement plan. The first is the virtual graph construction, the second is determining the maximum flow, and the third is the execution of the minimum-cost flow algorithm. Denoting $|V|$ and $|E|$ as the number of vertices and edges in the virtual graph, respectively, we have $|V| = O((\lceil\frac{D}{R}\rceil^2)(\lceil\frac{R}{d}\rceil)^2)$ and $|E| = O((\lceil\frac{F}{d}\rceil)(\lceil\frac{R}{d}\rceil)(\lceil\frac{D}{R}\rceil^2))$, where $\lceil\frac{D}{R}\rceil^2$ denotes the number of regions, $\lceil\frac{R}{d}\rceil^2$ denotes the number of subregions, and $\lceil\frac{F}{d}\rceil$ denotes the number of reachable regions for each region. The time complexity of the virtual graph construction is $O(|V| + |E|)$. The time complexity for determining the maximum flow using the implementation in [18] is $O(|V||E|^2)$ and the time complexity for determining the minimum cost flow using the implementation in [20] is $O(|V|^2|E|log|V|)$. As such, the resulting time complexity of our solution is $O(max(|V||E|^2, |V|^2|E|log|V|))$. We wish to emphasize here that the above implementations are not necessarily the fastest. For a detailed survey of other works on the maximum flow and minimum cost problems, please refer to [21] and [22].

4.4 Extending Our Solution for Multiple Flips

Our solution presented above considered sensors that can flip only once. We now discuss how to extend the above solution when a sensor can flip more than once. In this case, we only have to modify G_V to incorporate more *reachable* regions due to multiple flips. Let us consider the example in Fig. 4a. Let $F = d$ and let us assume that a sensor can flip to a distance d twice. For region 1 in Fig. 4a, its reachable regions now are regions 2, 3, 5, 6, and 9. Thus, edges are added from v^{out}_1 to v^{in}_2, v^{in}_3, v^{in}_5, v^{in}_6, and v^{in}_9. The edge capacity is still infinity for all the edges. The cost of the edge from v^{out}_1 to v^{in}_2 and v^{in}_5 is still one. However, since a sensor in region 1 needs two flips to move to regions 3, 6, and 9, the cost of the edges from v^{out}_1 to v^{in}_3, v^{in}_6, and v^{in}_9 is two. Correspondingly, edges are also added from v^{out}_2, v^{out}_3, v^{out}_5, v^{out}_6, and v^{out}_9 to v^{in}_1, with infinite edge capacity and appropriate edge costs. All other regions are treated similarly in G_V. The rest of the solution remains the same. It can be shown that the resulting movement plan is optimal (the proof is straightforward from Theorem 1).

4.5 Alternate Approaches to Execute our Solution

Our solution requires information on the number of sensors in each region in the network. In the above, we proposed letting a centralized base-station to collect this information and execute our solution. We now discuss distributed approaches to execute our solution. In the first approach, sensors in the network once again share information about the number of sensors in their regions. In the extreme case, a sensor in each region can execute our solution independently with this information. An alternate distributed approach is to divide the network into multiple areas. In this approach, we let each area obtain region information *only* in their area and not exchange it with other areas. A special sensor in each area can then execute our solution independently only with this information (without global synchronization with other areas) and determine a movement plan for sensors in its area. We call this the *area-based* approach. However, this approach can only achieve local optima in each area and cannot guarantee global optima in the sensor network. We will study the performance of this approach further using simulations in Section 5.

5 Performance Analysis

In the above, we proved the optimality of our solution in terms of coverage and number of flips. We now study the sensitivity of coverage and the number of flips to flip distance under different choices (for flip distance), initial deployment scenarios, and coverage requirements. We also study performance and overhead when our solution is executed using the area-based approach discussed in Section 4.5.

5.1 Performance Metrics and Evaluation Environment

Let the total number of regions in the network be Q. We denote Q_i as the number of regions with at least one sensor at initial deployment and denote Q_o as the number of regions with at least one sensor after the movement plan determined by our solution is executed. Our first metric is the Coverage Improvement, CI. Since, we already proved the optimality of final deployment, we want to study here the *improvements* in coverage as a result of executing our solution compared to initial deployment. Formally, $CI = Q_o - Q_i$. We define the Flip Demand as the number of flips required per region increase in coverage. The Flip Demand quantifies the efficiency of flips in improving coverage. Denoting J as the optimal number of flips as determined by our solution, we have $FD = \frac{J}{Q_o - Q_i}$. In order to compare the overhead of our optimal and area-based solution, we define the metric packet number PN incurred by the solutions. This metric is defined in Section 5.2.3 when we actually compare the two solutions.

We conduct the following simulations on two network sizes, 300×300 units and 150×150 units. The region sizes are $R = 10$ and $R = 20$ units. The basic unit of flip distance $d = 10$ units. We vary the flip distance F from 10 units to 40 units. The choices are $C = 1$ and $C = n$. Recall that if F is, say, 40 and $C = 1$, the flip distance for the sensors is fixed as 40 units. When $C = n$, we can have flip distances between 0 and F in discrete steps of the basic unit of flip distance d $(= 10$ units). Thus, if $F = 40$ $(4d)$, we have $C = 4$ and, in this case, sensors can flip to distances 10, 20, 30, and 40 units. The number of sensors deployed is equal to the number of regions. All data reported here were collected across 10 iterations, and averaged. Our implementations of the maximum flow algorithm is the Edmonds-Karp algorithm [18] and minimum cost flow algorithm is the one in [20]. We conduct our simulations using MATLAB. We use a topology generator for 2D-Normal distribution. The X and Y coordinates are independent of each other (i.e., $\sigma_x = \sigma_y$). We use $\sigma = \frac{1}{\sigma_x^2}$ to denote the degree of concentration of deployment in the center of the network field. Thus, larger values for σ implies more concentrated deployment in the center of the field. When $\sigma = 0$, the deployment is uniform.

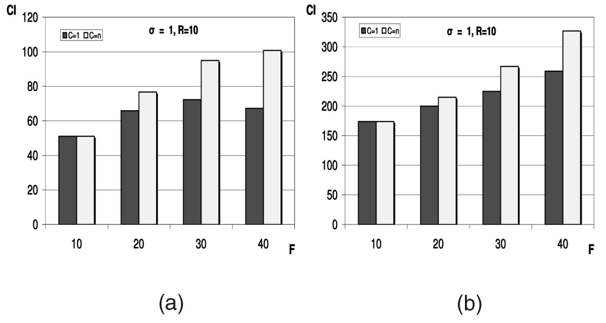

Fig. 6. Sensitivity of CI to F under different C in a 150×150 and 300×300 network.

5.2 Our Performance Results

5.2.1 Sensitivity of CI and FD to F under Different C

Figs. 6a and 6b show the sensitivity of CI to flip distance F under different choices C in two different network sizes (150×150 and 300×300), where $R = 10$, $\sigma = 1$, and $d = 10$. The number of regions in the networks are $15 \times 15 = 225$ and $30 \times 30 = 900$, respectively. We observe that, in both figures, for a given value of F, $C = n$ has larger CI compared to $C = 1$, except for $F = d = 10$, when both $C = n$ and $C = 1$ have the same performance. This is because, when $F = 10$, we have $n = 1$ and, so, $C = n$ is the same as $C = 1$. However, when $F > 10$, for a given F, there are more flip choices that our solution can exploit when $C = n$, hence increasing CI. The second observation we make is that when $C = n$, as F increases, CI increases in both figures. This is also because, when $C = n$, an increase in F means more choices to exploit. However, the trend is different when $C = 1$. In general, a large flip distance (even when $C = 1$) may appear to perform better as more far away holes can be filled if F increases. However, when $C = 1$, such improvements depend on the size of the network. Beyond a certain point (depending on the network size), an increase in F becomes counter-productive. This is due to two reasons. First, many sensors near the borders of the sensor network have flips that cannot be exploited when F is too large. Second, the chances of sequential flips (i.e., sensor x flipping to sensor y's region, sensor y flipping to sensor z's region, and so on) to cover holes are reduced when F is too large. The value of F, where this shift takes place in the 150×150 network in Fig. 6a, is $F = 40$, where CI decreases. Such a shift is not observed for the 300×300 network in Fig. 6b as the network size is quite large.

Figs. 7a and 7b show the sensitivity of flip demand FD to flip distance F under different choices C in two different network sizes. We wish to emphasize here that the number of flips does not linearly increase with coverage. Consequently, to enable a fairer comparison, we compare FD across different cases when the final coverage is the same. For both network sizes, we set $R = 10$ and $\sigma = 0$, where the

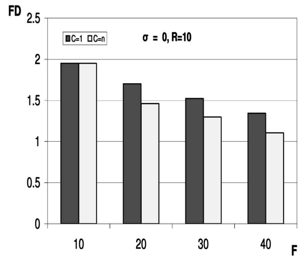

(a)

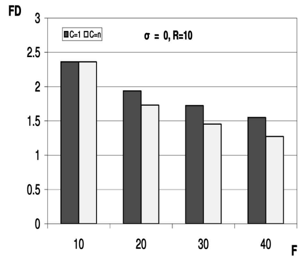

(b)

Fig. 7. Sensitivity of FD to F under different C in a 150 $\times$ 150 and 300 $\times$ 300 network.

final deployment covers *all* regions. Since the initial distribution is the same, the coverage improvement is the same. The comparison becomes more meaningful. From Figs. 7a and 7b, we see that, for a given value of F, $C = n$ has a lower FD than $C = 1$, except for $F = d = 10$, when both $C = n$ and $C = 1$ have the same performance. This observation is consistent with our earlier observations on CI. The second observation we make is that, as F increases, FD decreases, irrespective of C in both figures. When F is small, in order to achieve optimality, there may be multiple flips from sensors farther away from a hole (although the number of flips is still optimum). As F increases, it is likely that far away sensors can flip to such holes directly, minimizing the number of flips. By comparing Figs. 7a and 7b, we observe that FD is more for the 300 $\times$ 300 network compared to the 150 $\times$ 150 network. For a larger network with more regions, more flips have to be made. Consequently, FD is larger.

5.2.2 Sensitivity of CI to F under Different R and σ

Fig. 8 shows how the flip distance F impacts coverage improvement (CI) under different region sizes (R). Here, $\sigma = 1$ and $C = n$. In order to study the sensitivity of CI to region size fairly, the number of regions for different regions sizes should be the same. In Fig. 8, for a 150 $\times$ 150 and 300 $\times$ 300 network, we set the region sizes as $R = 10$ and $R = 20$, respectively. The number of regions in both cases is $15 \times 15 = 225$. We observe that, when flip distance (F) increases, CI is consistently better irrespective of R. When F increases, our solution can exploit more choices $(C = n)$ and CI increases. The second observation is that, as R increases, CI decreases. This is because, when R is small, neighboring regions are closer to each other (in terms of distance between the centers of the regions). For the same F, our solution is more likely to find sensors from other regions that can flip to fill holes. However, when R is large for the same F, the sensors that can flip from one region to another have to be relatively close to the borders of the regions. Thus, the number of sensors that can be found to flip is less. Naturally, CI (which captures improvement) decreases when R is large. Thus, performance improvement due to increases in flip distance is constrained by the desired region size.

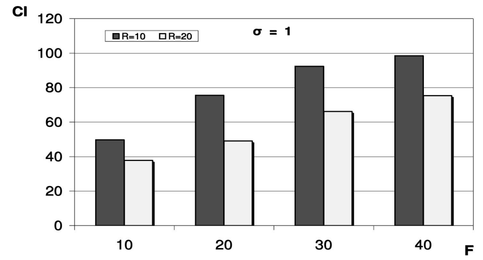

Fig. 8. Sensitivity of CI to F under different R.

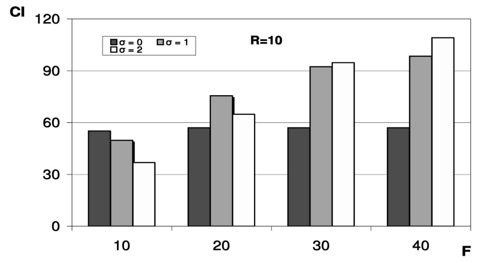

Fig. 9. Sensitivity of CI to F under different σ.

Fig. 9 shows how the flip distance F impacts CI under different distributions in initial deployment. The network size is 150 $\times$ 150, $R = 10$, and $C = n$. We vary σ from 0 (uniform distribution) to 4 (highly concentrated at the center of the field). The first observation we make here is that increases in flip distance (F) increases CI. However, the degree of increase in CI is impacted by σ. When $\sigma = 0$ (uniform), CI is almost the same for all values of F. This is because, in our simulations, close to full coverage is achieved when $\sigma = 0$. Since the initial deployment is the same for all cases, the improvement is the same.

We now study the trade-off between increasing F and σ in terms of which parameter has a more dominating effect on CI. In Fig. 9, when $F = 10$, σ dominates over F. We can see that, as σ increases (bias increases), CI deceases. The increase in bias cannot be compensated for by using sensors with flip distance of only 10 units. However, when F increases, our solution can exploit more choices $(C = n)$. Thus, F dominates when it increases. However, the degree of domination still depends on σ. When $F = 20$, $\sigma = 1$ performs better that $\sigma = 0$. This is because the increase in bias can be compensated for better when $F = 20$ (than was the case, when $F = 10$). Thus, CI increases. However, increasing σ beyond this point makes the bias dominate and, consequently, CI decreases. When $F > 20$, the increase in F consistently dominates the increase in bias (although the degree of domination is different), showing that performance improvement due to increases in flip distance is limited by initial deployment distribution.

5.2.3 Sensitivity of CI and PN to Area Size

Recall from Section 4.5 that an alternate approach to executing our solution is to divide the entire network into smaller areas and determine a movement plan in each area independently. We study this approach under two network sizes: 150 $\times$ 150 and 300 $\times$ 300. We set $R = 10$, $F = 20$, $C = n$, and $\sigma = 1$ for both cases. Thus, the number of regions are 225 and 900, respectively. We divide the networks into multiple areas. We denote the area size A as the number of regions along one dimension in each area.[6]

6. In both network sizes, for optimal solutions, the area size should be 15 and 30, respectively.

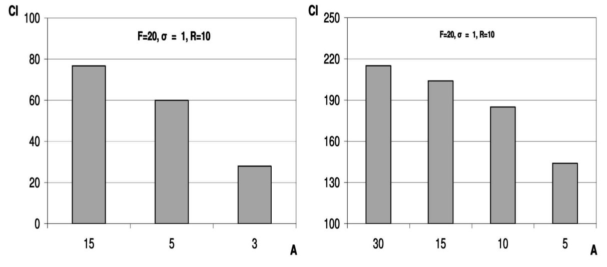

(a) (b)

Fig. 10. Sensitivity of CI to A in a 150 × 150 and 300 × 300 network.

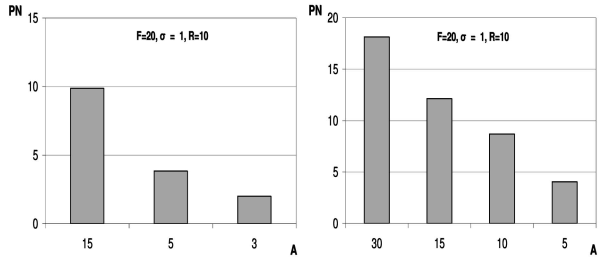

(a) (b)

Fig. 11. Sensitivity of PN to A in a 150 × 150 and 300 × 300 network.

We introduce a new metric here called packet number per region, PN. Denoting P as the total number of packets (or messages) sent and Q as the number of regions, we have $PN = \frac{P}{Q}$. The packet number quantifies the overhead incurred by the approaches. The packet number is calculated based on a simple protocol. After initial deployment, an elected region-head in each region sends a packet to the base-station (located in the center of the network) with information on the number of sensors in its region. The packets are forwarded along shortest paths through other regions. After the base-station receives all packets and determines a movement plan, it sends a packet to each region in the reverse path, informing sensors of their movement plan. A similar protocol is assumed for the area-based approach, where the region-head in each area will forward region information to a special sensor in the area, which executes the algorithm and forwards a movement plan to each region in the area. Note that there can be other versions of the above protocols, like direct relaying of messages, row-wise (or column-wise) message delivery, etc.

For the 150 × 150 network, we study CI and PN under three area sizes, namely, 15, 5, and 3. For the 300 × 300 network, we study CI and PN under four area sizes, namely, 30, 15, 10, and 5. From Figs. 10a and 10b, we can see that CI decreases as A decreases. When individual areas execute our solution independently, the areas can only achieve locally optimum solutions. However, we observe that, when the area size is half of the network size (i.e., $A = 15$ in Fig. 10b), CI is close to the globally optimum case. This is because of the exploitation of the bias in initial deployment. Since sensors are initially deployed one time targeted at the center of the network, the sensors are uniformly balanced in all directions surrounding the center. In this case, if we choose the area size as half the network size (resulting in four areas), we are optimizing deployment independently in the four directions from the center of the network. Since the sensors are uniformly balanced in all the four directions, the ensuing CI is not far from optimal (when $A = 15$ in Fig. 10b. Figs. 11a and 11b show the packet numbers for the optimal algorithm and the area-based approach. We can see that PN decreases as A decreases, demonstrating the savings in overhead in the area-based approach.

6 Discussions

Extensions to construct the virtual graph for any Region size R. In the above, we discussed the construction of the virtual graph when R was an integral multiple of d. In the following, we discuss the construction for any general value of R. Without loss of generality, let $R = sd + xd$, where s is an integer (≥ 0) and x is a real number ($1.0 \geq x \geq 0$). In the preceding cases, x was either 1.0 ($R = (s+1)d$) or 0 ($R = sd$). Let us now consider the case when ($1.0 > x > 0$). For two adjacent regions (say regions i and j), we cannot determine whether a sensor in region i can flip to region j in case $1.0 > x > 0$. To circumvent this problem, we leverage the concept of subregions. For each region of size R, we add a certain number of subregions of same size that meets the following condition; the size of each subregion should be a factor of d and a factor of R. In this situation, we can correctly determine if a sensor in a particular subregion can or cannot flip to another region. This can be done by traversing an integral number of subregions depending on d and the size of subregions. Our above solution is optimal if x is a terminating decimal. If x is nonterminating (e.g., $x = \frac{1}{3}$, $\frac{2}{3}$, etc.), we can choose an approximate subregion size such that the number of subregions is an integral multiple of R. The smaller the size of the subregion, the smaller the error from optimality is in this case.

Network partitions. In some situations, the network may be partitioned and we may need to repair them. In the approach proposed by Wu and Wang [2], empty holes are filled by placing a *seed* from a nonempty region to a hole. The algorithms to place seeds are tuned to meet load balancing objectives. We can apply the algorithms in [2] to repair partitions in our case. Once seeds are placed, our proposed solution can be executed. The key issue is the optimality of final coverage and the number of flips, given the mobility limitations of sensors. Developing optimal solutions for partition recovery problem using flip-based sensors is a part of our ongoing work.

Arbitrary flip directions. Our solution can be extended to handle situations where a sensor can flip to regions in arbitrary directions apart from left, right, top, and bottom directions. The *reachability* relationship between regions changes under arbitrary flip directions. In G_V, we have to add edges from each region to all newly *reachable* regions from it, corresponding to arbitrary directions of sensor flips.

Deployment under hostile zones/failures in Sensor Networks. In some cases, there may be certain hostile zones in the network (lakes, fires, etc.) that can destroy sensors. To avoid sensor flips to such zones, we only have to modify the edges and their capacities to such hostile zones in the virtual graph. The resulting solution is optimal.

In some cases, there can be faults/failures in the sensors and their communication. For example, if a sensor makes an erroneous movement to a region other than the intended region, there will be an extra hole in the network. Or, if a packet from a region does not reach the base-station, the region will be incorrectly treated as a hole, which may result in extra sensors in that region. As such, our solution can tolerate a degree of faults/failures in the network at a cost of optimality. A rigorous study of deployment under faults/failures will be part of future work.

7 Final Remarks

In this paper, we studied sensor network deployment using flip-based sensors. We proposed a minimum-cost maximum-flow-based solution to optimize coverage and the number of flips. We also proposed multiple approaches to execute our solution in practice. Our performance data demonstrated that, while increased flip-distances achieves better coverage improvement and reduces the number of flips required per region increase in coverage, such improvements are constrained by initial deployment distributions of sensors, due to the limitations on sensor mobility. In this paper, we considered sensors that can flip to distances in increments of a basic unit (d). We are currently working on continuous sensor mobility, although the overall movement distance (F) is still limited.

Appendix

Proof of Theorem 1 in Section 4.3

Proof. We first prove that our solution optimizes coverage. We prove by contradiction. Consider a flip plan W^S_{opt} in the sensor network corresponding to a flow plan W^V_{opt} in G_V obtained by our solution. Let W^S_{opt} be nonoptimal in terms of coverage. This means there is a better flip plan, W^S_x that can cover at least one extra region in the sensor network. Clearly, a corresponding flow plan W^V_x can be found in G_V. The amount of flow in W^V_x is larger than the maximum flow in W^V_{opt}. This is a contradiction.

We now prove that our solution optimizes the number of flips. We prove by contradiction. Consider a flip plan W^S_{opt} in the sensor network corresponding to a flow plan W^V_{opt} in G_V obtained by our solution. Let W^S_{opt} be nonoptimal in terms of the number of flips. This means there is a better plan, W^S_x, that can reduce at least one flip in the sensor network. Clearly, a corresponding flow plan W^V_x can be found in G_V. The number of flips in W^V_x is less than that in W^V_{opt}. This is a contradiction. □

Acknowledgments

This work was partially supported by the US National Science Foundation (NSF) under grant No. ACI-0329155 and CAREER Award CCF-0546668. Any opinions, findings, and conclusions or recommendations expressed in this material are those of the authors and do not necessarily reflect the views of NSF.

References

[1] A. Howard, M.J. Mataric, and G.S. Sukhatme, "Mobile Sensor Network Deployment Using Potential Fields: A Distributed, Scalable Solution to the Area Coverage Problem," *Proc. Int'l Symp. Distributed Autonomous Robotics Systems (DARS),* June 2002.

[2] J. Wu and S. Wang, "Smart: A Scan-Based Movement-Assisted Deployment Method in Wireless Sensor Networks," *Proc. IEEE INFOCOM,* Mar. 2005.

[3] T. Clouqueur, V. Phipatanasuphorn, P. Ramanathan, and K. Saluja, "Sensor Deployment Strategy for Target Detection," *Proc. ACM Int'l Conf. Wireless Sensor Networks and Applications (WSNA),* Sept. 2002.

[4] G. Wang, G. Cao, and T. La Porta, "Movement-Assisted Sensor Deployment," *Proc. IEEE INFOCOM,* Mar. 2004.

[5] A. Howard, M.J. Mataric, and G.S. Sukhatme, "An Incremental Self-Deployment Algorithm for Mobile Sensor Networks," *Autonomous Robots,* special issue on intelligent embedded systems, Sept. 2002.

[6] H. Zhang and J.C. Hou, "Maintaining Coverage and Connectivity in Large Sensor Networks," *The Wireless Ad Hoc and Sensor Networks: An Int'l J.,* Mar. 2005.

[7] Y. Zou and K. Chakrabarty, "Sensor Deployment and Target Localization Based on Virtual Forces," *Proc. IEEE INFOCOM,* Apr. 2003.

[8] S. Shakkottai, R. Srikant, and N.B. Shroff, "Unreliable Sensor Grids: Coverage, Connectivity and Diameter," *Proc. IEEE INFOCOM,* Apr. 2003.

[9] N. Bulusu, J. Heidemann, and D. Estrin, "Adaptive Beacon Placement," *Proc. IEEE Int'l Conf. Distributed Computing Systems (ICDCS),* Apr. 2001.

[10] http://www.darpa.mil/DARPATech2002/presentations/ato_pdf/speeches/ALTSCHUL.pdf, 2002.

[11] Y. Zou and K. Chakrabarty, "Uncertainty-Aware Sensor Deployment Algorithms for Surveillance Applications," *Proc. IEEE Global Comm. Conf. (GLOBECOM),* Dec. 2003.

[12] W. Heinzelman, A. Chandrakasan, and H. Balakrishnan, "Energy-Efficient Communication Protocol for Wireless Microsensor Networks," *Proc. Hawaii Int'l Conf. System Sciences (HICSS),* Jan. 2000.

[13] V. Isler, K. Daniilidis, and S. Kannan, "Sampling Based Sensor-Network Deployment," *Proc. IEEE/RSJ Int'l Conf. Intelligent Robots and Systems (IROS),* Sept. 2004.

[14] A. Howard, M.J. Mataric, and G.S. Sukhatme, "Relaxation on a Mesh: A Formation for Generalized Localization," *Proc. IEEE/RSJ Int'l Conf. Intelligent Robots and Systems (IROS),* Nov. 2001.

[15] B. Karp and H.T. Kung, "Greedy Perimeter Stateless Routing for Wireless Networks," *Proc. ACM Int'l Conf. Mobile Computing and Networking (MOBICOM),* Aug. 2000.

[16] P. Bose, P. Morin, I. Stojmenovic, and J. Urrutia, "Routing with Guaranteed Delivery in Ad Hoc Wireless Networks," *Proc. Int'l Workshop Discrete Algorithms and Methods for Mobile Computing and Comm.,* Aug. 1999.

[17] Y. Xu, J. Heidemann, and D. Estrin, "Geography-Informed Energy Conservation for Ad Hoc Routing," *Proc. ACM MOBICOM,* July 2001.

[18] T. Cormen, C. Leiserson, R. Rivest, and C. Stein, *Introduction to Algorithms.* MIT Press, 2001.

[19] A.V. Goldberg, "An Efficient Implementation of a Scaling Minimum-Cost Flow Algorithm," *J. Algorithms,* vol. 22, 1997.

[20] A.V. Goldberg and R. Tarjan, "Solving Minimum-Cost Flow Problems by Successive Approximation," *Proc. ACM Symp. Theory of Computing (STOC),* May 1987.

[21] A.V. Goldberg, "Recent Developments in Maximum Flow Algorithms," *Proc. Scandinavian Workshop Algorithm Theory (SWAT),* 1998.

[22] P.T. Sokkalingam, R.K. Ahuja, and J.B. Orlin, "New Polynomial-Time Cycle-Canceling Algorithms for Minimum-Cost Flows," *Networks,* vol. 36, pp. 53-63, 2000.

Sriram Chellappan received the bachelor's degree in instrumentation and control engineering from the University of Madras and the master's degree in electrical engineering from The Ohio State University. He is a graduate student in the Department of Computer Science and Engineering at The Ohio-State University. His current research interests are in network security, distributed systems, and wireless networks.

Xiaole Bai received the BS degree in the optical fiber communication field from the Electrical Engineering Department at Southeast University, China, in 1999 and the MS degree in communication and networking from the Helsinki University of Technology, Finland, in 2003. From September 2003 to September 2004, he worked as a research scientist in the Networking Lab at the Helsinki University of Technology. He is now working toward the PhD degree in the Computer Science and Engineering Department at The Ohio State University. His research interests include distributed computing, network architecture, and distributed algorithms.

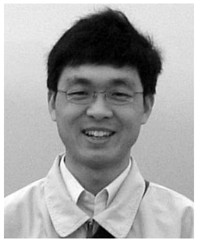

Bin Ma received the PhD degree from Peking University in 1999. He is a Canada research chair in bioinformatics and an associate professor in the Department of Computer Science at the University of Western Ontario. He was a recipient of the Ontario Premier's Research Excellence Award in 2003.

Dong Xuan received the BS and MS degrees in electronic engineering from Shanghai Jiao Tong University (SJTU), China, in 1990 and 1993, and the PhD degree in computer engineering from Texas A&M University in 2001. Currently, he is an assistant professor in the Department of Computer Science and Engineering, The Ohio State University. He was on the faculty of electronic engineering at SJTU from 1993 to 1997. In 1997, he worked as a visiting research scholar in the Department of Computer Science, City University of Hong Kong. From 1998 to 2001, he was a research assistant/associate in Real-Time Systems Group of the Department of Computer Science, Texas A&M University. He is a recipient of the US National Science Foundation (NSF) CAREER award. His research interests include real-time computing and communications, network security, sensor networks, and distributed systems. He is a member of the IEEE.

Changqing Xu received the MS and BS degrees in electronic engineering from Shanghai Jiao Tong University (SJTU) in 1993 and 1989, and he is currently pursuing the PhD degree in the same major. He is an associate professor and vice dean of the College of Electronic, Information, and Electrical Engineering at SJTU, China. His research interests are signal processing and mobile and wireless communications.